JOURNAL OF MATERIALS SCIENCE 31 (1996) 1707–1714

Mechanics of fibre fragmentation

A. N. GENT, Y.-W.CHANG
Institute of Polymer Engineering, The University of Akron, Akron, Ohio 44325-0301, USA
M. NARDIN, J. SCHULTZ
C.N.R.S. Centre de Recherches sur la Physico-Chimie des Surfaces Solides, 24 av. du President Kennedy, Mulhouse 68200, France

A fragmentation specimen consists of a single fibre embedded along the axis of a long narrow resin block. When the fibre is broken by a tensile load, either a lateral crack runs outwards into the resin, initiated by the break, or a debond (or equivalently a cylindrical crack in the resin) propagates along the fibre. Debonding always occurs with thin fibres. Strain energy release rates have now been calculated, analytically for long debonds and by FEA for short ones. The force to propagate a debond is found to increase as the debond grows, reaching a final value, termed "pull-out force", that is higher for softer fibres. If this force exceeds the strength of the fibre, then the fibre breaks again. This is the proposed mechanism of fibre fragmentation. For weakly-bonded, stiff fibres, the inferred minimum distance between breaks, i.e. the critical fragment length, is deduced to be of the order of the geometric mean of the radii of fibre and resin block, about 0.1–0.5 mm for typical fragmentation specimens, and it increases as the ratio of fibre stiffness to resin block stiffness increases, in agreement with observation.

1. Introduction

A common test for adhesion uses a single fibre embedded along the axis of a resin block. When a sufficiently large tensile force is applied to the specimen, parallel to the fibre, the fibre breaks repeatedly until it breaks no more. The average length of the resulting fragments, denoted l_c, is an inverse measure of adhesion; the smaller l_c, the greater is the inferred strength of adhesion between resin and fibre. From a balance of forces Kelly and Tyson [1] derived a relation between l_c and the shear stress τ_i causing failure at the interface:

$$l_c/r_f = \sigma_b/\tau_i \quad (1)$$

where r_f is the fibre radius and σ_b is the fibre breaking stress. However, the interfacial breaking stress τ_i is a somewhat ill-defined quantity that cannot be measured independently. Most adhesion tests are now interpreted instead in terms of a characteristic fracture energy G_a, defined as the energy required to propagate a debond through unit area of interface. For example, the pull-out force, F, for an inextensible rod or fibre of radius r_f embedded in an elastic block of cross-sectional area A_m is given by [2]:

$$F^2 = 4\pi r_f A_m E_m G_a \quad (2)$$

where E_m is the tensile (Young's) modulus of the resin block. If the strength of adhesion is high, then pull-out takes place by growth of a cylindrical crack in the resin, near the interface, instead of by debonding from the fibre. In this case G_a is replaced in Equation 2 by the fracture energy G_c of the resin. Additional work expended in frictional sliding can be included in the analysis, at least to a first approximation [3, 4]. We now seek to interpret fragmentation tests in a similar way, in terms of a fracture energy G_a or G_c.

After the fibre breaks, debonds or cracks in the resin near the interface are assumed to propagate along the fibre, away from the break. The force required to cause these cracks to propagate is assumed to increase as they grow in length, so that it eventually reaches a level at which the fibre breaks again somewhere else. This is the proposed mechanism of fragmentation. However, it requires a debonding ("pull-out") force that "rises" as the debonded length increases, whereas, according to Equation 2, the force required to propagate a debond along an embedded rod or fibre, starting from the embedded end, is "constant". Previous studies [3–5] have therefore focused on frictional contributions to the pull-out force, because they lead naturally to increasing force as the debond grows. (If the pull-out force does not increase there is no reason why a broken fibre should break again.) But the frictional contribution is small for small-radius fibres and for small debonds [4], and it seems too small to play an important role in fragmentation of fine fibres. Many technical fibres are only about 5 μm in radius and have fragmentation lengths of only about 0.5–1 mm. It seems unlikely in these cases that subsequent fractures are caused by a frictionally-induced rise in pull-out force. In order to account for repeated fracture of the fibre another mechanism must be invoked for an increase in pull-out force as debonding proceeds. We have now carried out finite element

0022–2461

analysis (FEA) on fine fibres in the early stages of debonding, in order to examine the relation between pull-out force and debond length. The results are reported here.

Data on typical fragmentation lengths can be obtained from the literature. For single glass fibres embedded in epoxy resin, DiBenedetto and Lex [6] reported values of l_c in the range 0.15 to 0.55 mm. Bascom and Jensen [7] reported fragment lengths in the range 0.2 to 1 mm for various carbon fibre/epoxy combinations. Baxevanakis *et al.* [8] obtained average fragmentation lengths of about 0.25 mm for a similar system. Netravali *et al.* [9] obtained values in the range 0.4 to 1.2 mm for a glass fibre/epoxy system, using fibres with radii between 5 and 13 μm. Thus, for typical combinations of fibre and resin, fragment lengths are typically between 0.1 and 1 mm. From studies over a much broader range of resins, however, Asloun *et al.* [10] concluded that the critical fragmentation length is related to the ratio of Young's (tensile) modulus E_f of the fibre to the modulus E_m of the resin, as well as to the interfacial bond strength. For well-bonded systems, in which failure probably took place in the resin, rather than at the interface, they found that log (l_c/r_f) increased linearly with log (E_f/E_m), with a slope of about 0.5. However, two different relations were obtained:

$$l_c/r_f = 9.4\,(E_f/E_m)^{1/2} \quad (3)$$

for stiffer glassy and thermoplastic resins, and

$$l_c/r_f = 1.3\,(E_f/E_m)^{1/2} \quad (4)$$

for elastomeric resins. Although a dependence on elastic moduli would be expected, these particular results have not been accounted for theoretically up to now.

Recently, Gent and Wang [11, 12] studied two modes of failure after an embedded fibre breaks: interfacial debonding or cracking, leading to pull-out of the fibre, and lateral cracking of the resin block causing fracture of the specimen. For inextensible fibres they showed that pull-out was preferred for small-radius fibres, even when the bond strength had the maximum possible value, equal to the fracture energy G_c of the resin itself, whereas lateral cracking was preferred for large-radius fibres. But they did not consider the question: why do fibres break repeatedly? We now take up this question again, and use similar FEA methods to investigate the mechanics of fracture of a single-fibre specimen in which the fibre radius is extremely small in comparison with the width and thickness of the resin block, as is customary in fragmentation tests. The compliance of the fibre is therefore comparable to that of the resin even though its tensile modulus may be much higher.

2. Theoretical considerations

2.1. Interfacial failure

For an inextensible fibre embedded in a block of an elastic resin the pull-out force is given in Equation 2. If the fibre is extensible, however, energy is stored in it as well as in the resin. For a long thin specimen, Fig. 1,

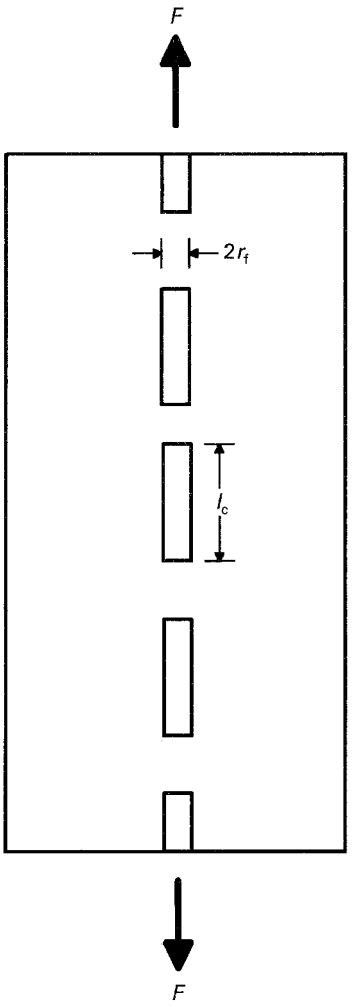

Figure 1 Sketch of fragmentation specimen with a broken fibre.

equal tensile strains e_b are set up in both fibre and resin in the still-bonded portion of the specimen, and a larger tensile strain e_u is set up in the unbonded resin portion, where e_b and e_u are given by

$$e_b = F/(A_f E_f + A_m E_m) \quad (5)$$

and

$$e_u = F/A_m E_m \quad (6)$$

where A_f and A_m denote the cross-sectional areas of fibre and resin, respectively. If they are both cylindrical, then $A_f = \pi r_f^2$ and $A_m = \pi(r_o^2 - r_f^2)$. Elastic moduli are E_f for the fibre and E_m for the resin.

Strain energy ΔW is imparted to the specimen when a further length Δc is debonded, where

$$\Delta W/\Delta c = F\,(e_u - e_b)/2 \quad (7)$$

and fracture energy of amount ΔW_a is expended, where

$$\Delta W_a/\Delta c = 2\pi r_f G_a \quad (8)$$

Pull-out of the fibre will occur when the work done, given by $F(e_u - e_b)\,\Delta c$, is as large as $\Delta W + \Delta W_a$. Thus, from Equations 5–8, the reduced pull-out force F^*, defined as $F/(E_m G_a)^{1/2}$, is given by

$$F^{*2} = 4\pi r_f A_m[1 + \alpha^{-1}] \quad (9)$$

where α denotes the relative stiffnesses of fibre and matrix:

$$\alpha = A_f E_f / A_m E_m \quad (10)$$

Note that Equation 2 is recovered when $\alpha \gg 1$, i.e. when the stiffness of the fibre is much greater than that of the resin. On the other hand when the fibre is not much stiffer than the resin the pull-out force is greater than Equation 2 would predict, tending to infinity for relatively soft fibres.

An alternative way of stating Griffith's energy criterion for fracture employs the rate of change of the elastic compliance C of the specimen with length c of debond [13]:

$$F^2 = 4\pi r_f G_a (dC/dc)^{-1} \quad (11)$$

This formulation is particularly suitable for use with FEA because the compliance of complex systems is readily evaluated. It is employed here to treat the case of debonds that are small relative to the radius r_o of the specimen, when the assumptions on which Equations 2 and 9 are based no longer apply.

2.2. Fibre fracture

When the stress in the fibre rises to the breaking stress σ_b, it will break again. This will occur when $\sigma_b = E_f e_b$, where e_b is given in terms of the applied force F by Equation 5. Thus, the applied force at which the fibre will break again is that at which the pull-put force, given by Equation 11, reaches a critical value F_b, given by

$$F_b = \pi r_f^2 \sigma_b [1 + \alpha^{-1}] \quad (12)$$

2.3. Matrix cracking

Results have been obtained previously for the force required to make a circular crack grow outwards into the resin from a break in an inextensible fibre [11, 12]. The force is given by:

$$F^2 = 4\pi a G_c (dC/da)^{-1} = 4\pi a (r_o - r_f) E G_c / f \quad (13)$$

where a is the radius of the crack, G_c is the fracture energy of the resin and f is given by

$$f = \frac{d(CE)}{d[(a - r_f)/(r_o - r_f)]} \quad (14)$$

The crack propagation force F increases as the crack radius a increases until the crack reaches a critical size, about half way to the outer radius of the specimen. After that, the crack grows catastrophically. Thus, the breaking force is rather high for tough resins and largely independent of the initial crack radius (i.e. the fibre radius) [11, 12]. As shown below, it is also not much affected by extensibility of the fibre. Thus, for fibres of small radius, failure will always occur either by debonding or resin fracture close to the fibre, resulting in pull-out. The question is: how frequently will a fibre break during pull-put? What is the fragmentation length?

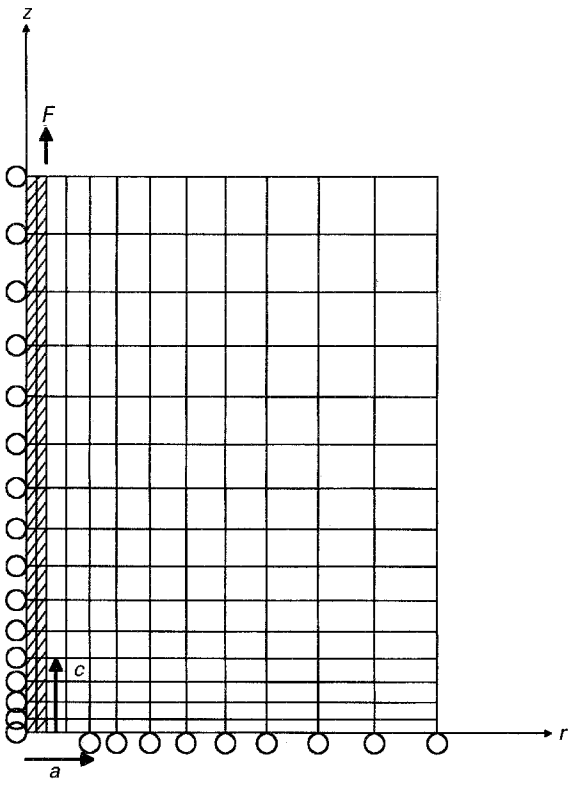

Figure 2 Representative grid used for FEA.

3. FEA modelling

Calculations were carried out using the ADINA FEA code [14], with the grid shown in Fig. 2. Because of symmetry, only one-half of the specimen was modelled. The external radius r_o of the resin block was chosen to be 3 mm in all cases and the half-length of the sample was taken be 25 mm. Fibres having three different radii were examined: 435, 25 and 5 μm. Axisymmetric quadrilateral 8-noded elements, with 9 integration points, were used; 15 elements in the radial direction and 50 in the length direction for fibres having a radius of 435 and 25 μm, and 19 in the radial direction and 40 in the length direction when the fibre radius was only 5 μm. The elements were discretized using logarithmic scales in both the axial and radial directions, with the size of the first element in the axial direction chosen to be about 20% of the fibre radius and in the length direction equal to the fibre radius. For inextensible fibres only one element was employed to characterize the fibre in the radial direction. For extensible fibres two radial elements were employed. Both the resin and the fibre were assumed to be isotropic, incompressible and linearly-elastic.

To represent inextensible fibres, Young's modulus E_f was made several orders of magnitude higher than that of the resin: nine orders higher for $r_f = 435$ μm, eleven orders higher for $r_f = 25$ μm and twelve orders higher for $r_f = 5$ μm. For extensible fibres, values of Young's modulus E_f were assigned of 10^2 and 10^3 times that of the resin for fibres with radius $r_f = 25$ μm, and 10^5 times for $r_f = 5$ μm.

In evaluating the compliance C of a specimen containing an inextensible fibre, a tensile load was applied to the upper end of the fibre without any constraints.

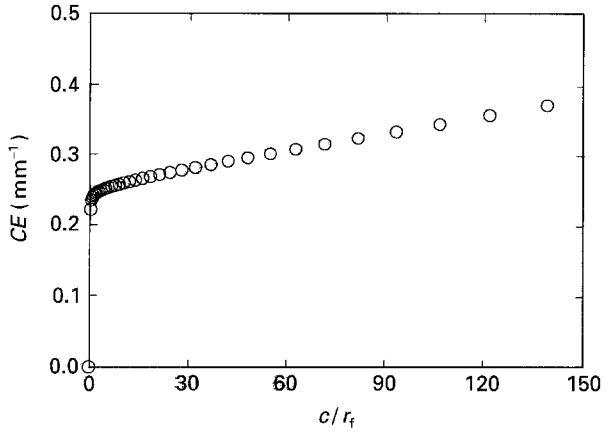

Figure 3 Compliance C versus debond length c for a typical specimen ($r_f = 25$ μm; $r_o = 3$ mm). E denotes the resin tensile (Young's) modulus.

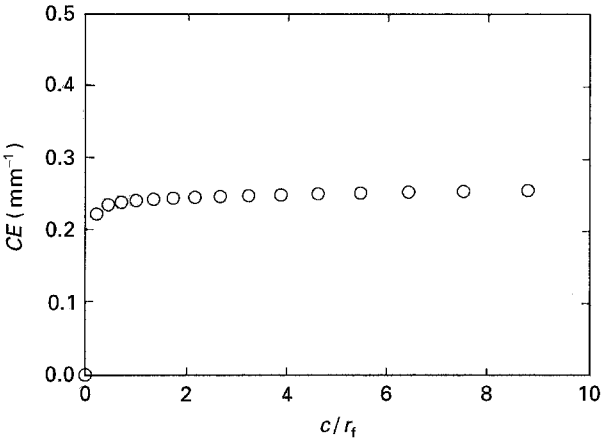

Figure 4 Expanded view of initial region of Fig. 3.

When the fibre was relatively extensible, however, the load was applied to one of the fibre nodes on the upper surface and all nodes on the upper surfaces of both the fibre and the resin block were constrained to undergo the same vertical displacement. To allow interfacial debonding, contact elements were employed at the fibre–resin interface, with zero friction. The sample compliance C was then calculated for different lengths c of debond and the results utilized in Equation 10 to calculate the reduced fracture force F^* [$= F/(E_m G_a)^{1/2}$]. Values of G_a and G_c have been made equal, giving the interface the maximum possible strength.

4. Results and discussion

4.1. Pull-out of inextensible fibres

A typical relation between compliance and crack length c is shown in Figs 3 and 4 for samples with

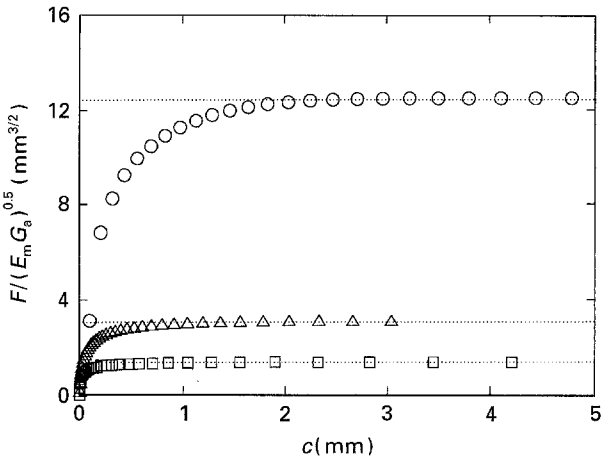

Figure 5 Reduced force required to propagate a debond as a function of debond length c for various fibre radii r_f. Squares, $r_f = 5$ μm; triangles, $r_f = 25$ μm; circles, $r_f = 435$ μm. $r_o = 3$ mm.

$r_f = 25$ μm and $r_o = 3$ mm. The compliance increased dramatically in the beginning and then, for longer debonds, increased linearly with length c of debond. Values of the reduced pull-out force F^* [$= F/(E_m G_a)^{0.5}$] were calculated by means of Equation 11 from the slope of the compliance relations. They are plotted against debond length in Fig. 5. Final pull-out values obtained in this way increased with fibre radius r_f. Values from FEA and from Equation 2 are compared in Table I: good agreement was found.

Calculated compliances increased rapidly for small crack lengths, suggesting that the initial force is zero. This becomes clearer when the initial region is magnified, Fig. 4. Gent and Wang [12] obtained small but non-zero values of the initial debonding force by extrapolating calculated forces for debonds of finite length back to a zero length (see Table 3 in [12]). However, this procedure is inexact for a relatively coarse grid. The present results, obtained with a more refined FEA grid, indicate that the initial value is indeed zero, as would be expected on theoretical grounds.

4.2. Matrix cracking

Calculated values of compliance are plotted against radius a of a circular resin crack in Fig. 6 for specimens with $r_f = 25$ μm and $r_o = 3$ mm. Corresponding forces required to propagate the crack were calculated from Equations 13 and 14. Reduced forces F^* ($= F/(E_m G_{a,c})^{1/2}$) for resin cracking are compared with those for fibre debonding in Figs 7, 8 and 9. Values of G_a and G_c have been made equal to give the interface the maximum possible strength.

TABLE I Comparison of F^* ($= F/(E_m G_a)^{0.5}$) for long debonds from FEA and from theory for different fibre radii

r_f (μm)	r_o (mm)	E_f/E_m	F^* (FEA) (mm$^{3/2}$)	F^* (Equation 2) (mm$^{3/2}$)	Relative error (%)
5	3	10^{12}	1.335	1.33	0.376
25	3	10^{11}	3.05	2.98	2.349
435	3	10^{9}	12.4	12.29	0.895
25	1	10^{11}	1.02	0.99	3.030

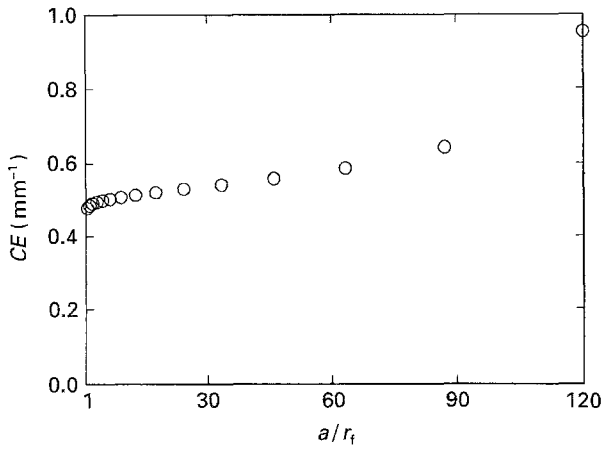

Figure 6 Compliance C versus crack radius a for a circular crack growing outwards into the resin. $r_f = 25$ μm; $r_o = 3$ mm. E denotes the tensile (Young's) modulus of the resin.

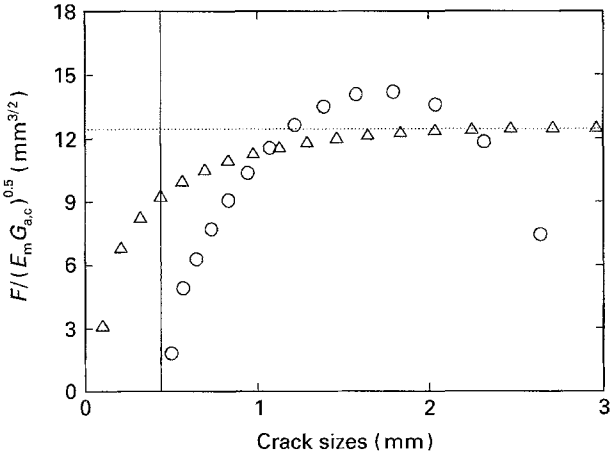

Figure 7 Reduced force (circles) required to propagate a lateral crack of radius a compared to the reduced force (triangles) required to propagate a debond of length c along the fibre. $r_f = 435$ μm; $r_o = 3$ mm.

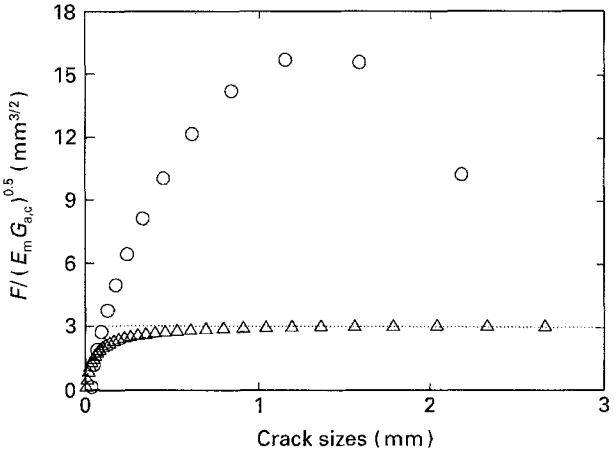

Figure 8 Reduced force (circles) required to propagate a lateral crack of radius a compared to the reduced force (triangles) required to propagate a debond of length c along the fibre. $r_f = 25$ μm; $r_o = 3$ mm.

In all cases the force required to propagate a resin crack outwards increased as the crack grew and reached a maximum value (termed "breaking force") at a point approximately half-way to the edge of the specimen, as found before, and in good agreement with experiment [12]. The breaking force did not vary significantly with fibre radius, Table II, in contrast to the pull-out force which increased markedly as the radius increased, as discussed in the preceding section. However, the pull-out force was always smaller than the breaking force. We conclude that, for these small-radius fibres, failure will always occur by growth of a debond or cylindrical crack along the fibre interface, rather than by lateral cracking of the specimen.

Again, as for growth of a crack outwards into the resin, the present results suggest that the force required to initiate a debond at the broken fibre ends is actually zero, rather than the small finite values deduced previously using a coarser grid [12].

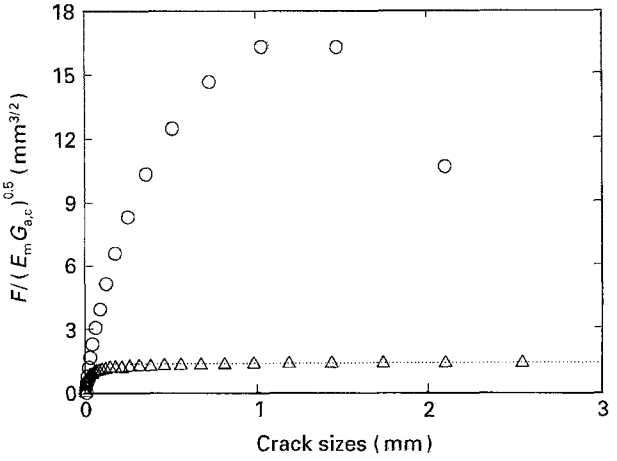

Figure 9 Reduced force (circles) required to propagate a lateral crack of radius a compared to the reduced force (triangles) required to propagate a debond of length c along the fibre. $r_f = 5$ μm; $r_o = 3$ mm.

TABLE II Reduced breaking forces $F^*_b (= F_b/(E_m G_c)^{1/2})$ for matrix cracking

r_f (μm)	F^*_b (mm$^{3/2}$)
5	16.27
25	15.68
435	14.17

4.3. Debonding of extensible fibres: pull-out or fragmentation

In Figs 10 and 11 the reduced pull-out force $F/(E_m G_a)^{0.5}$ is shown as a function of debond length for samples with $r_f = 25$ μm, $r_o = 1$ mm and $r_f = 5$ μm, $r_o = 3$ mm, and various values of the stiffness ratio $\alpha = r_f^2 E_f / r_o^2 E_m$. When α is reduced, i.e. when the fibre is made more extensible, the force required to propagate a long debond is increased. Final values F_p obtained by FEA are compared with those predicted by Equation 9 in Table III. Good agreement is seen to hold.

Relative values of the force required to propagate a debond, represented by the ratio F/F_p, are plotted against length c of debond in Fig. 12. The small debond region is magnified in Fig. 13. The shapes of the curves are quite similar. Indeed, when the debond length c is referred to a reduced mean radius r^*, given

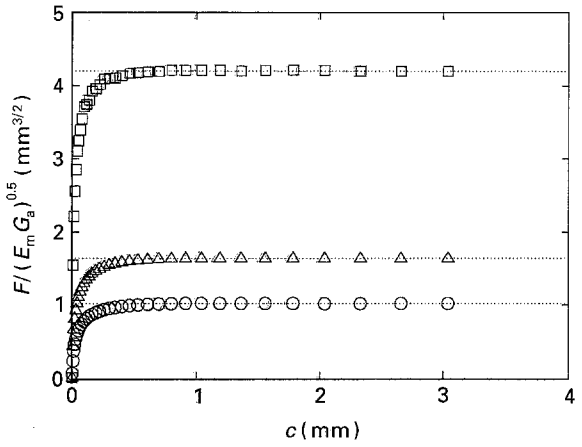

Figure 10 Reduced force to propagate a debond of length c, for various values of the ratio E_f/E_m of fibre and resin moduli. Squares, $E_f/E_m = 10^2$; triangles, $E_f/E_m = 10^3$; circles, $E_f/E_m = 10^{11}$. $r_f = 25$ μm; $r_o = 1$ mm.

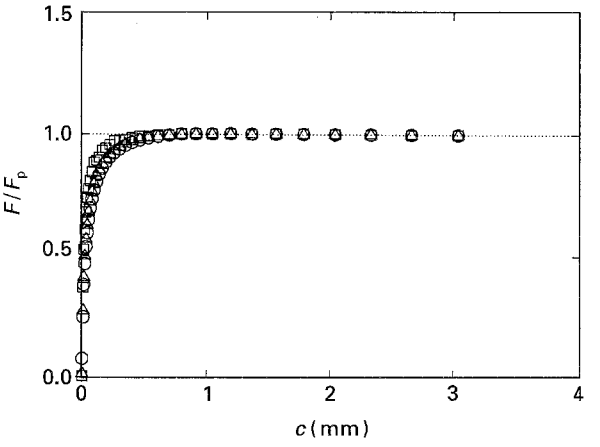

Figure 12 Force to propagate a debond of length c, relative to the maximum value, for various ratios E_f/E_m of fibre and resin moduli. Squares, $E_f/E_m = 10^2$; triangles, $E_f/E_m = 10^3$; circles, $E_f/E_m = 10^{11}$. $r_f = 25$ μm; $r_o = 1$ mm.

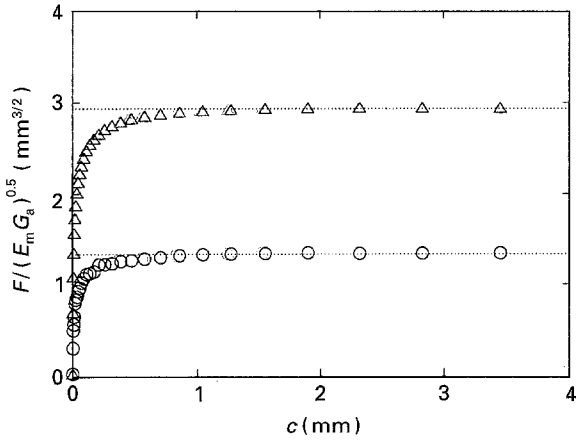

Figure 11 Reduced force to propagate a debond of length c, for various values of the ratio E_f/E_m of fibre and resin moduli. Triangles, $E_f/E_m = 10^5$; circles, $E_f/E_m = 10^{12}$. $r_f = 5$ μm; $r_o = 3$ mm.

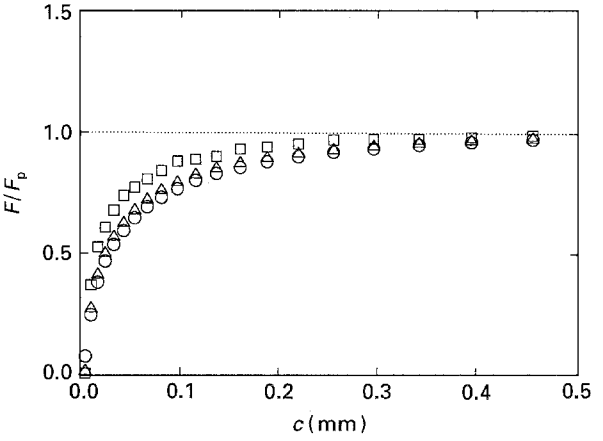

Figure 13 Magnified view of Fig. 12 for short debonds. Squares, $E_f/E_m = 10^2$; triangles, $E_f/E_m = 10^3$; circles, $E_f/E_m = 10^{11}$. $r_f = 25$ μm; $r_o = 1$ mm.

by the geometric mean of the fibre radius r_f and the radius r_o of the resin block in which it is embedded:

$$r^* = (r_f r_o)^{1/2} \quad (15)$$

then the curves form a single curve approximately, as shown in Fig. 14, for different radii of fibre and block. An empirical relation, found to fit all of the results approximately, is shown as the full curve in Fig. 14:

$$F/F_p = \tanh [1.5 (c/r^*)^{1/2}] \quad (16)$$

The pull-out force is seen to increase up to a debond length of about $2r^*$ and then it becomes virtually constant. If the fibre is inextensible and the radius r^* is relatively large, as considered previously [11, 12], then the pull-out force will be small in comparison to the expected strength of the fibre and the fibre will be pulled out without breaking. However, if the fibre radius r_f is only a few microns, then the final pull-out force may be greater than the fibre can withstand. In this case the fibre will break when the debond has grown only a small distance. Successive fractures of this kind are thought to be the mechanism of fibre fragmentation.

A debond can grow from both ends of a fibre fragment. Thus, a fragment will break again if its length is more than twice the length of debond at which a constant pull-out force is achieved (and that force is greater than F_b). We conclude from Fig. 14

TABLE III Reduced values of final pull-out force for debonding extensible fibres

r_f (μm)	r_o (mm)	E_f/E_m	F^* (FEA) (mm$^{3/2}$)	F^* (Equation 9) (mm$^{3/2}$)	Relative error (%)
5	3	10^5	2.93	2.86	2.45
25	1	10^2	4.21	4.09	2.93
25	1	10^3	1.645	1.60	2.81

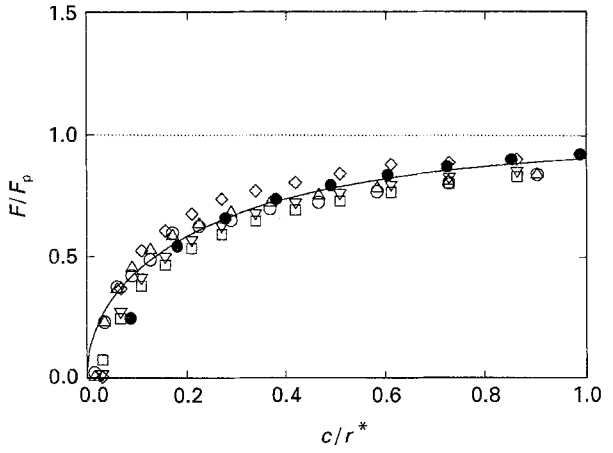

Figure 14 Force to propagate a debond, relative to the maximum value, versus debond length c, relative to the geometric mean radius r^* of fibre and resin block, for various fibre radii and modulus ratios E_f/E_m. Full curve: $F/F_p = \tanh [1.5\ (c/r^*)^{1/2}]$. $r_f = 5$ μm, $r_o = 3$ mm; $E_f/E_m = 10^5$, △; $E_f/E_m = 10^{12}$, ○. $r_f = 25$ μm, $r_o = 1$ mm; $E_f/E_m = 10^2$, ◇; $E_f/E_m = 10^3$, ▽; $E_f/E_m = 10^{11}$, □. $r_f = 435$ μm, $r_o = 3$ mm; $E_f/E_m = 10^9$, ●.

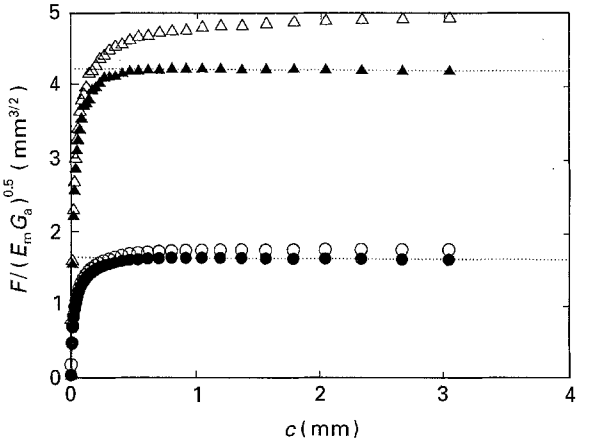

Figure 15 Effect of number n of radial grid elements in fibre on debond force F. Open symbols, $n = 1$; filled, $n = 2$. $r_f = 25$ μm; $r_o = 1$ mm. Triangles, $E_f/E_m = 10^2$; circles, $E_f/E_m = 10^3$.

that fragment lengths l_c will be about $5r^*$ at most, or about 500 μm for a fibre of radius 5 μm embedded in a resin block of radius 2 mm. If a debond can grow to this size under a force less than F_b, then the fibre will pull out without breaking again. On the other hand, if the interface is relatively strong, then the force to propagate a debond will be greater and the fibre will break again when the debond has grown only a short distance along the fibre. In this case the final fragment length will be correspondingly short. Thus, an inverse relation is expected between fragment length, taken as twice the debond length, and fracture energy G_a for the interface. And the computed fragment lengths are comparable to, although somewhat smaller than, those observed in practice, i.e. about 0.2 to 1 mm for fibres of a few μm in radius, embedded in a long resin block of 1–2 mm in width and thickness. Thus, the present analysis appears to account for the general features of fragmentation observed with fine fibres.

It should be mentioned that the final value of the fracture force, especially for extensible fibres, depended on details of the FEA grid employed. When only one element was used to represent the fibre radius the pull-out force did not reach a constant value at large debonds and the values were larger than predicted by Equation 9, Fig. 15. Adding one more element improved the results, but there was still about 3 per cent error for large debonds. It is thought that the results have a similar accuracy for other sizes of debond also, but it would clearly be better to use still more elements to represent an extensible fibre.

4.4. Effect of stiffness ratio α on fragment length

An implicit relation between fragment length and fracture energy of the interface is contained in the empirical relation, Equation 16, found to hold between applied force F and debond length or crack length c. Fracture of the fibre will occur when F reaches the value F_b at which the stress on the fibre exceeds its breaking stress. (We assume for simplicity that F_b is given by Equation 12, although this relation will be strictly correct only when the fibre fragment length is much greater than the mean radius r^*.) Taking the applied force F to be a significant fraction, say one-half, of the final pull-out force F_p, Equations 12 and 16 are found to yield large values of fragment length only when the fibre is much stiffer than the matrix, $\alpha \gg 1$. For relatively soft fibres the predicted debonded length is extremely small, comparable to the fibre radius. This conclusion appears to hold over a wide range of possible values for the interfacial fracture energy G_a. However, although the fragment length is predicted to increase with modulus ratio α, in accord with the experimental observations of Asloun *et al.* [10] and Nardin *et al.* [15], it is not known to what extent the fracture energy G_a of the interface was also changed in their experiments. Quantitative comparison of predicted fragment lengths with experimentally-observed values is therefore not feasible. We can conclude only that an increase in fragment length with both modulus ratio and ratio of cross-sectional area of fibre and resin is to be expected, and that in the extreme case of stiff, weakly-bonded fibres, the fragment length becomes many times larger than the fibre radius (as is commonly observed), eventually reaching a value of the order of the mean radius r^* of fibre and resin block.

5. Conclusions

1. Pull-out forces have been calculated for fibres having relatively long debonded lengths, for various ratios α of fibre stiffness to resin stiffness. It is concluded that pull-out forces are greater for softer fibres.

2. Applied forces at which a small debond will propagate have also been calculated by FEA. They increase as the length of debond increases to reach a final value (the pull-out force) when the debond length is comparable to the geometric mean radius r^* of the fibre and resin block in which the fibre is embedded.

3. Assuming that the fibre breaks before the final (pull-out) force is reached, values of the fragment

length l_c, taken as twice the debond length, are predicted to fall somewhat below 500 μm for fibres of typical radii, 5 μm, embedded in resin blocks of typical width and thickness, 2 mm. Thus, the general order of magnitude of observed lengths of fibre fragments is in accord with the hypothesis that the fibre breaks again when the applied force required to propagate a debond along the fibre reaches a sufficiently high value.

4. When the stiffness of the fibre is comparable to or less than that of the resin block, it is concluded that fibre fragments could become extremely small in length, of the order of the radius of the fibre. In these circumstances the assumptions on which the analysis is based will cease to hold. (Moreover, even if such small fragments were formed, they might pass unnoticed.)

References

1. A. KELLY and W. R. TYSON, *J. Mech. Phys. Solids* **13** (1965) 329.
2. A. N. GENT, G. S. FIELDING-RUSSELL, D. I. LIVINGSTON and D. W. NICHOLSON, *J. Mater. Sci.* **16** (1981) 949.
3. A. N. GENT and G. L. LIU, *ibid.* **26** (1991) 2467.
4. A. N. GENT and O. H. YEOH, *ibid.* **17** (1982) 1713.
5. A.N. GENT and S. Y. KAANG, *Rubber Chem. Technol.* **62** (1989) 757.
6. A. T. DIBENEDETTO and P. J. LEX, *Polym. Eng. Sci.* **29** (1989) 543.
7. W. D. BASCOM and R. M. JENSEN, *J. Adhesion* **19** (1986) 219.
8. C. BAXEVANAKIS, D. JENLIN and D. VALENTIN, *Comp. Sci. Tech.* **48** (1993) 47.
9. A. N. NETRAVALI, P. SCHWARTZ and S. L. PHOENIX, *Polym. Compos.* **10** (1989) 385.
10. E. I. M. ASLOUN, M. NARDIN and J. SCHULTZ, *J. Mater. Sci.* **24** (1989) 1835.
11. A. N. GENT and C. WANG, *J. Mater. Sci.* **27** (1992) 2539.
12. *Idem, ibid.* **28** (1993) 2494.
13. J. G. WILLIAMS, "Fracture Mechanics of Polymers" (Wiley, New York, 1984) p. 30.
14. K. J. BATHE, "ADINA: A Finite Element Program for Automatic Dynamic Incremental Non-Linear Analysis", Report No. 82448-1 (Massachusetts Institute of Technology, Cambridge, Massachusetts, 1987).
15. M. NARDIN, A. EL MALIKI and J. SCHULTZ, *J. Adhesion* **40** (1993) 93.

Received 12 January
and accepted 15 August 1995